

# The role of Harper–Dorn creep at high temperatures and very low stresses

Praveen Kumar · Michael E. Kassner ·  
Terence G. Langdon

Received: 7 April 2008 / Accepted: 25 April 2008 / Published online: 21 May 2008  
© Springer Science+Business Media, LLC 2008

**Abstract** Creep experiments were conducted on single crystals of very high purity aluminum to evaluate the validity of the Harper–Dorn region of flow which occurs at very low stresses and high homologous temperatures. The results confirm the existence of a different flow process under these conditions but with a stress exponent closer to  $\sim 3$  rather than 1. Measurements show that the dislocation density within this low stress region varies with stress in a manner consistent with the behavior anticipated from an extrapolation of data reported in the regime of conventional power-law creep at high stresses. All of the experimental results are in reasonable agreement with earlier published data, including with the original data of Harper and Dorn when their results are plotted without incorporating a threshold stress.

## Introduction

It is now well-established that the creep rate,  $\dot{\epsilon}$ , occurring under steady-state conditions in high temperature flow is

dependent upon the applied stress,  $\sigma$ , the absolute testing temperature,  $T$ , and the grain size of the material,  $d$ , through a relationship of the form [1, 2]

$$\dot{\epsilon} = \frac{ADG\mathbf{b}}{kT} \left(\frac{\mathbf{b}}{d}\right)^p \left(\frac{\sigma}{G}\right)^n \quad (1)$$

where  $D$  is the appropriate diffusion coefficient (equal to  $D_o \exp(-Q/RT)$ , where  $D_o$  is the frequency factor,  $Q$  is the activation energy, and  $R$  is the gas constant),  $G$  is the shear modulus of elasticity,  $\mathbf{b}$  is the Burgers vector,  $k$  is Boltzmann's constant,  $p$  and  $n$  are the exponents of the inverse grain size and the stress, respectively, and  $A$  is a dimensionless constant. It follows from Eq. (1) that, for any selected material and creep testing conditions, the strain rate is determined exclusively by the values of  $Q$ ,  $n$ ,  $p$ , and  $A$ .

Following Eq. (1), experimental creep data are generally presented on logarithmic coordinates as the measured creep rate versus the applied stress, where the slope of this type of plot defines the magnitude of the stress exponent,  $n$ . Over a range of intermediate stresses, experiments on numerous pure metals and metallic alloys show that the creep properties typically lead to stress exponents lying within the range from 3 to  $\sim 6$ , where an exponent of  $n = 3$  is associated with a dislocation glide process [3] and higher values of  $n$  are associated with control by a dislocation climb process [4] where the precise value of the stress exponent is dependent upon the stacking-fault energy of the material. Experimental variations in the values of  $n$  in this regime of intermediate stresses are associated with well-established transitions between the glide and climb processes in the creep of solid solution alloys where solutes can segregate preferentially to the dislocations [5, 6]. Similar types of power-law creep are also observed over wide ranges of stress in ceramic materials [7, 8].

---

P. Kumar · M. E. Kassner · T. G. Langdon (✉)  
Departments of Aerospace & Mechanical Engineering  
and Materials Science, University of Southern California,  
Los Angeles, CA 90089-1453, USA  
e-mail: langdon@usc.edu

T. G. Langdon  
Materials Research Group, School of Engineering Sciences,  
University of Southampton, Southampton SO17 1BJ, UK

*Present Address:*

P. Kumar  
Department of Mechanical and Astronautical Engineering,  
Naval Postgraduate School, Monterey, CA 93943, USA

Although this region of power-law behavior typically extends over a very wide range of stresses, at very low stresses there is generally a transition to a flow regime in which the stress exponent has a lower value and may be equal to 1. This region of Newtonian viscosity is generally associated with the occurrence of diffusion creep in which plastic flow arises through the diffusion of vacancies from areas having high vacancy concentrations to areas having low vacancy concentrations. If the diffusion of vacancies occurs through the crystalline lattice the process is known as Nabarro–Herring diffusion creep [9, 10] and if diffusion occurs along the grain boundaries it is known as Coble diffusion creep [11]. The basic principles of these two processes are now well-understood and they both lead to flow occurring by Eq. (1) with  $n = 1$  but with  $D = D_\ell$  and  $p = 2$  for Nabarro–Herring creep and  $D = D_{gb}$  and  $p = 3$  for Coble creep where  $D_\ell$  and  $D_{gb}$  are the diffusion coefficients for lattice and grain boundary diffusion, respectively.

An important contribution in the field of high temperature creep occurred in 1957 when Harper and Dorn [12] reported experimental data for pure (99.99%) aluminum that were not consistent with the predictions of Nabarro–Herring creep when conducting experiments at a very high temperature of 920 K corresponding to an homologous temperature of  $\sim 0.99 T_m$  where  $T_m$  is the absolute melting temperature of the material. Shortly thereafter, similar creep data were reported by Barrett et al. [13] and Mohamed et al. [14] from experiments also conducted on pure aluminum.

The results from these three sets of experiments are shown in Fig. 1 where Eq. (1) has been rearranged so that the temperature-compensated creep rate,  $\dot{\epsilon}kT/DG\mathbf{b}$ , is plotted against the normalized stress,  $\sigma/G$ : these results are plotted by putting  $D$  equal to the coefficient for lattice self-diffusion given by  $D_\ell = 1.86 \times 10^{-4} \exp(-143,400/RT) \text{ m}^2 \text{ s}^{-1}$  for pure aluminum [15] with  $G = \{(3.022 \times 10^4) - (16.0 \times T)\} \text{ MPa}$  for pure aluminum [15],  $\mathbf{b} = 2.86 \times 10^{-10} \text{ m}$  and with the double-shear testing data of Mohamed et al. [14] converted to normal stresses and normal strain rates using  $\sigma = 2\tau$  and  $\dot{\epsilon} = 2\dot{\gamma}/3$  where  $\tau$  and  $\dot{\gamma}$  are the shear stress and the shear strain rate, respectively. Following the procedure adopted by Harper and Dorn [12], the results from their experiments are plotted in Fig. 1 in terms of the applied stress minus a measured threshold stress.

Several conclusions may be reached from inspection of Fig. 1. First, the experimental data show a conventional regime with  $n \approx 4.5$  at the higher stresses but at low stresses, equivalent to normalized stresses of  $\sigma/G < 10^{-5}$ , there is a transition to a well-defined region with  $n \approx 1.0$ . Second, all three sets of data are consistent, within the limits of experimental scatter, in this low stress region which extends through more than one order of magnitude

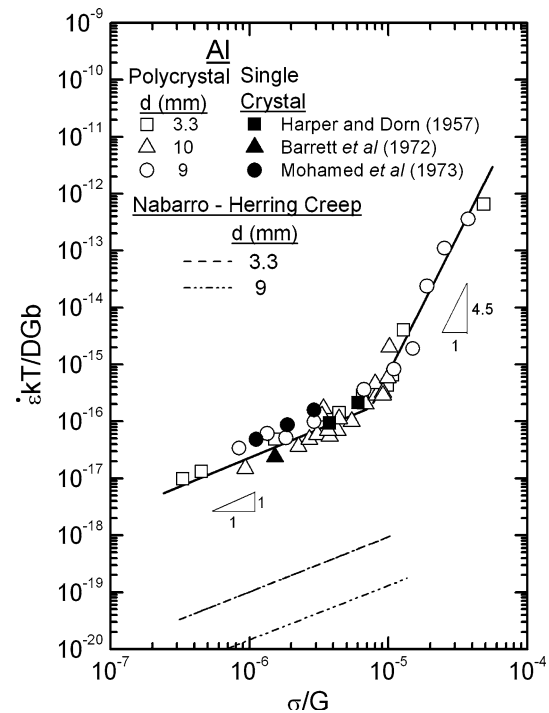


**Fig. 1** Normalized creep rate versus normalized stress showing the early evidence for the occurrence of H–D creep [12,13,14] and the predictions for Nabarro–Herring diffusion creep [9,10]: for the results of Harper and Dorn [12], the values of stress denote the applied stress minus a measured threshold stress

of normalized stress. Third, the results in the low stress region are in agreement both for different polycrystalline grain sizes of 3.3 and 9 or 10 mm and for data, shown by the solid points, collected on single crystals. This agreement between large-grained polycrystalline samples and single crystals demonstrates that flow in this region has no dependence on grain size so that  $p = 0$  in Eq. (1). Fourth, and most important, creep occurs in this region at rates which are very significantly faster than the rates predicted by Nabarro–Herring diffusion creep. This is illustrated by the two lower lines which delineate the predicted rates for Nabarro–Herring creep with grain sizes of 3.3 and 9 mm, respectively. Thus, there is a discrepancy between the predicted diffusional flow rate and the results obtained by Harper and Dorn [12] of more than two orders of magnitude and there are even larger discrepancies for the other two sets of data. It is important to note also that Coble diffusion creep predicts even slower creep rates under these conditions.

The results of Harper and Dorn [12] firmly established the possibility of a new and heretofore undefined creep mechanism occurring at low stresses and very high temperatures and this creep behavior was later designated Harper–Dorn (H–D) creep. Numerous subsequent experiments have attempted to check or verify the occurrence of

H–D creep and a detailed summary of these various data was given in a recent review [16]. In broad terms, and concentrating exclusively on experimental data reported for metals at very high testing temperatures, there are several results that are reasonably consistent with the occurrence of H–D creep because they confirm the presence of a region having a lower value of  $n$  at low stresses [17–27] but there are also other results where there is no deviation to a region having a lower stress exponent at low stresses so that they appear to negate the occurrence of H–D creep [28–31].

The present experiments were initiated to address and resolve the origins of this apparent dichotomy. Specifically, the objective was to carefully conduct a series of long-term creep tests at a high temperature and very low stresses, to record the variation of creep strain as a function of time, to deduce the steady-state creep rates and to make a direct comparison with the published data. In view of the various differences and discrepancies which are documented in the published literature, a critical first-step was to select the test material and to establish a well-defined and precise testing procedure that avoided, as far as possible, any ambiguities that may be inherent in the testing process. Accordingly, the following section describes the testing material and the creep testing routine, the next section delineates the experimental results and the following section compares the present data with results available in the published literature.

## Experimental material and procedures

### Selection of the test material

All of the creep tests were conducted using very high purity (99.999%) aluminum single crystals. Aluminum was selected to provide a direct comparison with the very early data summarized in Fig. 1. In addition, a very high purity was an important prerequisite because earlier work by Mohamed and coworkers [22, 24, 25] showed the occurrence of H–D creep in polycrystalline Al of 99.999% purity but an absence of H–D creep when the purity was reduced to 99.99%. It is important to note in this respect that Harper and Dorn [12] reported the use of polycrystalline Al with a purity of 99.99% but Mohamed [27] noted recently that the purity may have been higher than originally reported and/or the dislocation density may have been very low after annealing, where the latter condition is also conducive to the occurrence of H–D creep. Single crystals were selected for two reasons. First, the absence of grain boundaries necessarily precludes both the influence of Nabarro–Herring diffusional creep and the occurrence of any erroneous effects due to grain growth. Accordingly, it is reasonable to

assume that any experimental deviation to a lower stress exponent in single crystals at low stresses is due unambiguously to the occurrence of an intragranular dislocation flow process. Second, it is reasonable to anticipate a consistency with H–D creep when using aluminum single crystals because the very early data also included some limited tests on Al single crystals as shown by the solid points in Fig. 1. All of the single crystals were creep tested in compression using samples having a [100] orientation parallel to the compressive axis. This orientation was selected because it gives eight separate slip systems having a Schmidt factor of  $\sim 0.41$  thereby providing a potential for more uniform deformation by comparison with other orientations.

The single crystal material was provided by MaTeck GmbH (Juelich, Germany). A spectrographic analysis revealed the following impurities in ppm: Na 0.5, Zn 0.5, Mn 0.2, Si 1.0, Cu 1.0, Ti 0.2, Mg 1.0, Fe 2.0, and Cr 0.2. The as-received material was in the form of a long cylindrical rod having a diameter of 25 mm and a length of 125 mm. A large diameter was selected specifically to minimize any size effects or adverse effects due to surface oxidation.

An important additional consideration in compression testing is the shape, and especially the height to diameter ratio, of the creep samples. It is well-established that if the height to diameter ratio is high then the samples will deform by buckling whereas if the ratio is low, as with cubic samples, the flow behavior is influenced by end effects due to the restricted slip occurring in the areas where the sample surfaces impinge on the loading platens [32]. For the present tests, the rod of single crystal was glued within a special brass holder using a nonreactive polymer and cylindrical samples were then cut using a slow-speed saw having a thickness of 0.5 mm. Both flat ends were subsequently ground on grit papers to ensure they were perpendicular to the long axis. The cylindrical creep samples had aspect ratios, corresponding to the height/diameter dimensions, between  $\sim 1.6$  and 1.7. Finally, the samples were electro-polished at room temperature using a solution of 10% perchloric acid and 90% acetone.

Prior to creep testing, the samples were placed in the creep testing facility and annealed in air at 913 K for  $\sim 50$  h under a very low load of  $\sim 0.0002$  MPa. This low load was needed to maintain contact between the sample and the loading platens. The annealing was conducted both to remove any stress effects that may have been introduced during the sample preparation and to ensure a very low dislocation density since this is an important prerequisite for the occurrence of H–D creep [24, 27].

By carefully following these various steps, it is reasonable to assume that the test samples were in an ideal

condition to reveal the presence or absence of H–D creep in subsequent compression testing at low stresses and very high temperatures.

### Creep testing

All of the creep tests were conducted in air at a temperature of 913 K, with the temperature continuously monitored and maintained constant at the desired value to within  $\pm 1$  K. This temperature corresponds to  $0.98 T_m$  and it is similar to the temperatures used in many other investigations of H–D creep. Ceramic  $\text{Al}_2\text{O}_3$  platens were inserted in the creep testing facility immediately above and below the test sample and boron nitride was used as a lubricant between the sample and the platens in order to reduce any frictional effects. The creep testing facility operated under conditions of constant load but the absence of constant stress conditions is not significant at the very low strains inherent in these experiments. By using the boron nitride lubricant at either end of the sample, it was confirmed that there was very little barreling of the specimens at least over the strains incorporated in these tests.

Due to the very low stresses employed in these experiments (typically  $\sim 10^{-6}$  to  $10^{-5}$  G), extreme care was needed in order to obtain an accurate measure of the creep strain. Accordingly, almost all tests used a laser system to provide a continuous measure of the creep strain throughout each test. For this procedure, two  $\text{TiO}_2$  strips were placed on the sample surface close to and parallel to the upper and lower edges of the sample and the separation between these strips was taken as the gauge length for subsequent strain measurements. A boron window in the furnace wall permitted the laser beam to impinge directly onto the sample. The displacement between the  $\text{TiO}_2$  strips was measured using the laser and this information was used as input for a computer to provide a continuous permanent record of the strain displacement. In some early tests, the strain was measured using a regular linear voltage displacement transducer attached close to the ends of each sample. There were no apparent differences between these two types of measurement.

Several of the tests were conducted using a single constant load. Some additional tests were also conducted where the stress was changed abruptly either upward or downward during the test. Both types of testing yielded similar results and there were no apparent differences in the measured steady-state strain rates.

### Microstructural study

In order to observe the dislocation microstructure associated with creep at very low stresses, etch pit studies were conducted on both annealed samples and samples

deformed under creep conditions. All microstructural observations were performed on the [100] plane.

All samples were electropolished at room temperature using 90% acetone and 10% perchloric acid and they were then etched for 6–8 s using a solution of 50% HCl, 47%  $\text{HNO}_3$ , and 3% HF. The etched surfaces were observed using an optical microscope at various magnifications. In order to minimize the introduction of any artifacts, the etching was always performed immediately following the electropolishing. Typical photomicrographs of the etched surfaces were recorded both at randomly selected points and along linear traverses. These photomicrographs were used to provide a measure of the dislocation density,  $\rho$ , through the relationship [33]

$$\rho = \frac{2N}{A'} \quad (2)$$

where  $N$  is the total number of etch pits appearing within an area  $A'$ .

## Experimental results

### Creep properties

Creep tests were conducted over a range of stresses to include both the power-law regime where  $n = 4.5$  but with special emphasis on the low stress region where there is a potential for achieving H–D creep.

Figure 2 shows an example of a test conducted with stress changes where (a) shows the creep strain as a function of the testing time and (b) replots the data in terms of the instantaneous strain rate as a function of the strain,  $\epsilon$ . Although this test shows almost an immediate steady-state condition from zero strain at the lower stress of 0.03 MPa, several tests showed the occurrence of short regular primary stages of creep in which the strain rate gradually decreased to an essentially steady-state value. This behavior is consistent with many earlier experiments under similar testing conditions including in the earliest experiments by Harper and Dorn [12]. Several conclusions may be drawn from the data in Fig. 2. First, the creep behavior is regular and consistent even up to a strain of  $>0.012$  and for times up to  $\sim 5 \times 10^6$  s corresponding to  $\sim 58$  days. Second, similar strain rates are achieved when the stress is cycled upward and downward between different values as, for example, between 0.046 and 0.058 MPa. This reproducibility with strain confirms that flow is occurring under reasonably steady-state conditions. Third, the transient following the initial increase in stress from 0.03 to 0.046 MPa is consistent with the transients observed in conventional power-law creep for pure Al tested under conditions where dislocation climb is the rate-controlling

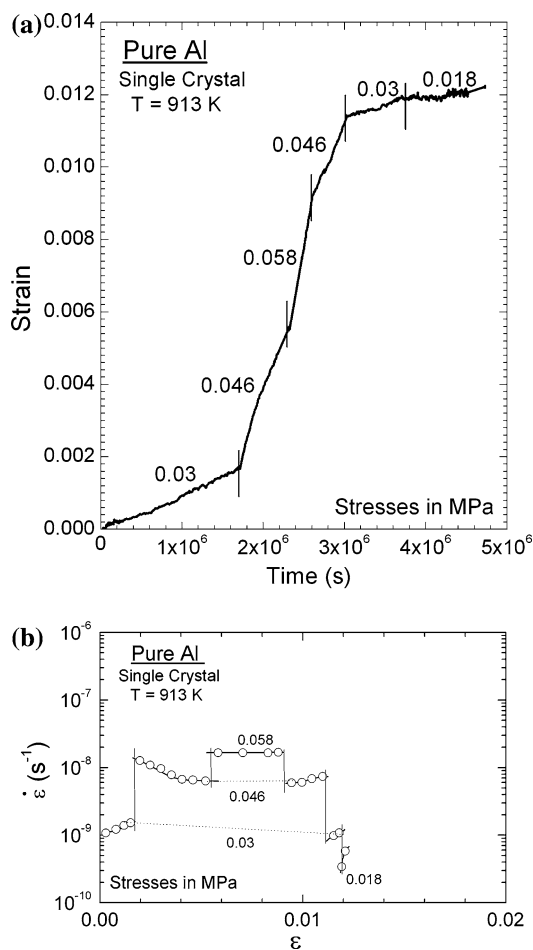


**Fig. 2** (a) Strain versus time for a single crystal tested in compression at 913 K with abrupt changes in the applied stress and (b) the corresponding plot of the instantaneous strain rate versus strain

process [34]. The presence of this transient suggests, therefore, the occurrence of some form of dislocation flow process.

The experimental data are recorded in Fig. 3 in a logarithmic plot of steady-state creep rate versus stress. Also included in Fig. 3 are the line delineating the anticipated behavior for dislocation power-law creep with  $n = 4.5$  at 913 K and the line delineating the behavior for H–D creep. Three conclusions may be drawn from these results. First, all of the results are mutually consistent and the small experimental scatter is less than a factor of 2 on the strain rate axis. Second, the points recorded at the highest stresses lie along the anticipated line with  $n = 4.5$ , thereby confirming the occurrence of dislocation climb as the rate-controlling process at the highest stresses. Third, there is a clear deviation from the line for  $n = 4.5$  at stresses lower than  $\sim 0.1$  MPa and within this low stress regime the stress exponent is close to  $\sim 3.1$ . It is reasonable to conclude that these results at the lower stresses represent a genuine creep behavior because earlier experiments on large-grained

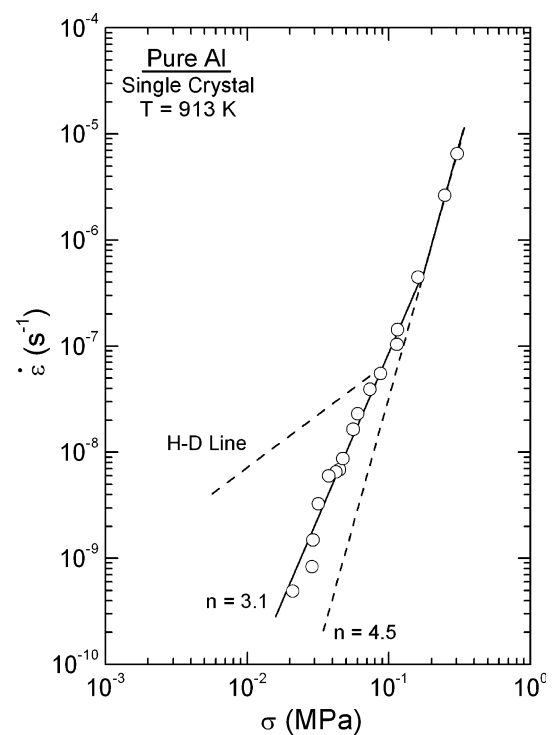


**Fig. 3** Steady-state creep rate versus stress for tests conducted on very high purity aluminum single crystals at 913 K

polycrystals using the same experimental facility gave datum points lying along the  $n = 4.5$  line even at creep rates down to  $\sim 10^{-9} \text{ s}^{-1}$  [35]. These latter results are reasonable for the large-grained polycrystals because the purity of these samples were only 99.97% and this level of purity is insufficient to reveal the H–D creep regime at the lowest stresses [27].

### Microstructural observations

Microstructural observations were undertaken to measure the dislocation densities in samples tested within the low stress regime. These measurements are important because early data by Barrett et al. [13] suggested the dislocation density may remain reasonably constant and independent of the applied stress within the H–D region.

An example of the etch pits revealed after creep testing is shown in Fig. 4 for a sample tested to a strain of 0.05 through stresses of 0.075, 0.120, 0.068, and 0.095 MPa, respectively. A first important observation is that no subgrains were visible in any of the specimens prepared by etching after creep testing within the low stress region. The results for the dislocation densities are shown in Fig. 5 plotted as the dislocation density,  $\rho$ , versus the normalized stress,  $\sigma/G$ ; also included in Fig. 5 are various other sets of data reported after testing pure Al both within and outside of the H–D region [13, 14, 22, 36, 37] and Al-5% Zn

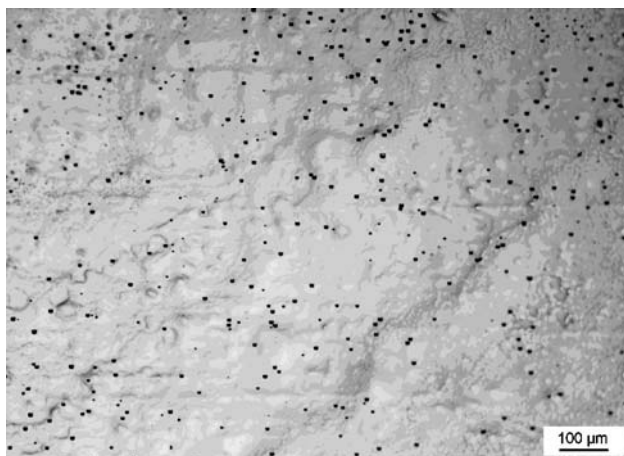


**Fig. 4** Etch pits in a sample tested to a strain of 0.05 through stresses of 0.075, 0.120, 0.068, and 0.095 MPa, respectively

outside of the H–D region [38], where the vertical broken line denotes the anticipated transition from H–D creep to conventional power-law creep with  $n = 4.5$ . In the present investigation, etching revealed both a set of relatively large well-defined etch pits and also many smaller etch pits that were less well-defined. However, individual measurements of the large pits and of all pits showed that both sets of datum points varied with stress in essentially an identical manner. Figure 5 also includes the measurements of Barrett et al. [13] which purport to show a dislocation density that is independent of stress within the H–D region.

It is apparent that all of the datum points in Fig. 5, including the present results for very high purity Al single crystals, lie within a narrow band that extends to the measurements recorded in the conventional 5-power-law

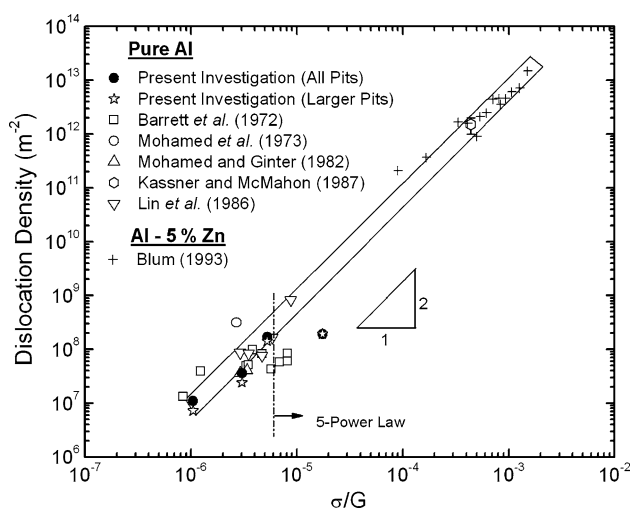


**Fig. 5** Dislocation density versus normalized stress showing data measured in the present experiments and in other experiments on pure Al [13, 14, 22, 36, 37] and Al-5% Zn [38]

region at high stresses for the Al-5% Zn alloy [38]. Since this plot has a slope of 2, it follows that the dislocation density is given by

$$\rho = \Psi \left( \frac{\sigma}{Gb} \right)^2 \quad (3)$$

where  $\Psi$  is a constant. Equation (3) was first derived in a detailed analysis of data from high temperature creep experiments by Bird et al. [1] where it was shown that the value of  $\Psi$  is of the order of  $\sim 1$  for a number of different metals. A similar value of  $\Psi \approx 1$  was derived also for ceramics and geological materials [8]. For the present experiments shown in Fig. 5,  $\rho \approx 10^7 \text{ m}^{-2}$  when  $\sigma/G \approx 10^{-6}$  so that, incorporating the Burgers vector of  $\mathbf{b} = 2.86 \times 10^{-10} \text{ m}$ , it follows that  $\Psi \approx 1$  which is in excellent agreement with these earlier studies that were taken outside of the H–D region.

Although the early data of Barrett et al. [13] suggested a constant dislocation density within the H–D region, the present results suggest instead that the dislocation density decreases with decreasing stress within this new creep region and these dislocation densities are fully consistent with those anticipated in conventional power-law creep.

## Discussion

The results from the present tests, conducted on very high purity aluminum single crystals, reveal the presence of a new creep regime at the lowest stresses but the results differ from conventional H–D creep because the stress exponent is closer to  $n \approx 3$  rather than  $n = 1$ . It is important therefore to compare these results with the earlier published data obtained in the testing of Al samples. The following section provides a direct comparison with the early data of Harper and Dorn [12] and the two subsequent sections compare these results with earlier data that were either not consistent with, or consistent with, the occurrence of H–D creep.

### Comparison with the data of Harper and Dorn [12]

In order to make a direct comparison between the present results and those of Harper and Dorn [12], it is first necessary to normalize all of the results to a single testing temperature. It is evident from Eq. (1) that, since the value of  $G$  cancels when  $n = 1$ , the temperature dependence of the creep rate is determined exclusively by the relevant values of the diffusion coefficient,  $D$ , where this neglects the trivial dependence on temperature incorporated within the term of  $1/T$ . Taking  $D = D_\ell$  and using the value for  $D_\ell$  given earlier [15], the present creep data and the results of Harper and Dorn [12] were normalized to a representative temperature of 923 K.

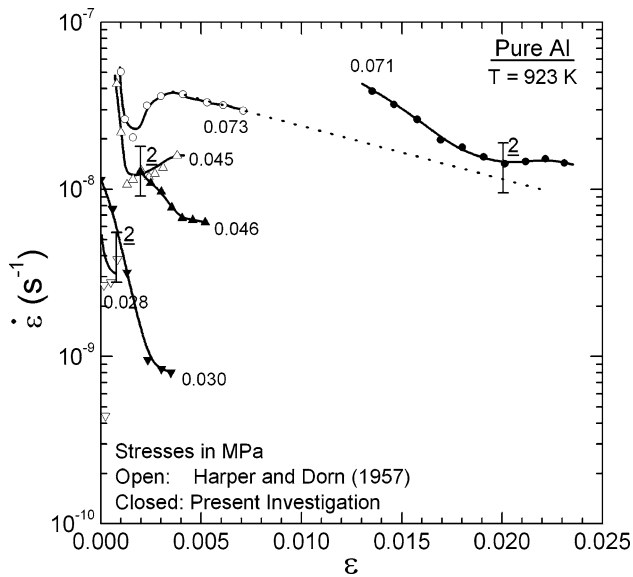


**Fig. 6** Instantaneous strain rate versus strain for tests conducted in the present investigation and in the early experiments of Harper and Dorn [12] with the data normalized to a temperature of 923 K

Figure 6 shows a direct comparison between the early data of Harper and Dorn [12] and the present experiments plotted in the form of the instantaneous creep rate against the measured strain, where the vertical lines labeled 2 denote a variation by a factor of two in strain rate for two sets of tests conducted at almost identical applied stresses. It should be noted that most of the early tests by Harper and Dorn [12] were extended only to total strains of less than 0.01 whereas the present experiments were continued to higher strains. Nevertheless, despite the severe limitation on strain in the work of Harper and Dorn [12], there is an excellent consistency between these two sets of data. Thus, at an applied stress of 0.071 MPa the present results are consistent with an extrapolation of the early data obtained at an applied stress of 0.073 MPa. Similarly, at 0.030 MPa in the present investigation the strain rates are consistent with the data of Harper and Dorn [12] at a stress of 0.028 MPa but the earlier tests were terminated at a very low strain and therefore the measured minimum strain rate was higher than the steady-state creep rate recorded in the present investigation.

The general consistency between the early data of Harper and Dorn [12] and the present results when plotted, as in Fig. 6, as strain rate versus strain for individual samples suggests there should be a correlation between the two sets of measured creep rates when plotted in the conventional form as strain rate versus normalized stress. The result is shown in Fig. 7 where the open circles denote the present data and the remaining points are taken from the investigation of Harper and Dorn [12] using two different plotting routines. In the original work of Harper and Dorn,

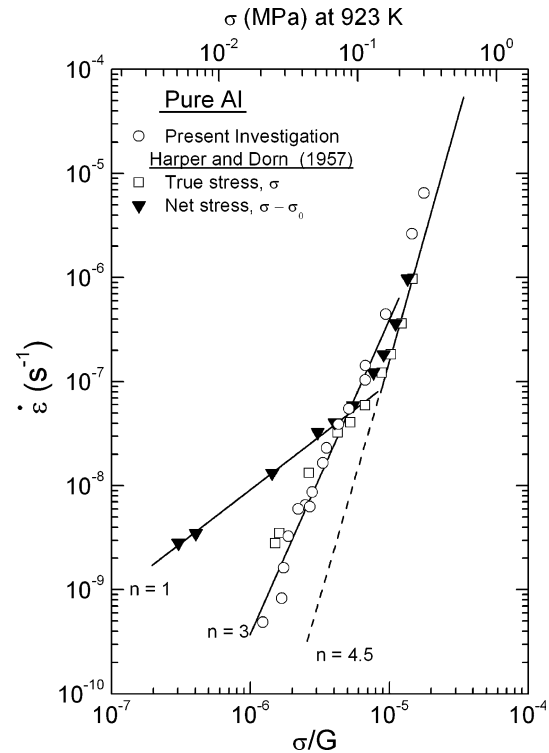


**Fig. 7** Steady-state creep rate versus normalized stress for the present results and the early data of Harper and Dorn [12] with and without the incorporation of a threshold stress,  $\sigma_0$

they reported the occurrence of a negative strain at a tensile stress,  $\sigma_0$ , of  $\sim 0.02$  MPa and accordingly they concluded there was a threshold stress due to the presence of a surface tension effect between the surface of aluminum, an oxide layer of  $\text{Al}_2\text{O}_3$  and the surrounding air. In order to avoid this problem, they plotted their creep data in terms of the creep rate versus the net stress acting on the samples,  $(\sigma - \sigma_0)$ . These points are shown by the solid inverted triangles in Fig. 7 and they delineate the classic region of H–D creep with a slope of  $n = 1$ . It is apparent that these results are reasonably consistent with the present data at values of  $\sigma$  above  $\sim 0.1$  MPa but at lower stresses there is a marked deviation between the two sets of data.

In the present experiments there was no evidence for any threshold stress and this was demonstrated by plotting strain rate against stress on linear axes and showing the data extrapolate to zero strain rate at zero stress. However, the incorporation of a threshold stress into the plot of Harper and Dorn [12] has a critical effect on the data because the value of  $\sigma_0$  becomes of major significance at these very low stresses. This is illustrated in Fig. 7 where the same creep data of Harper and Dorn [12] are replotted in terms of the true applied stress,  $\sigma$ , as shown by the open squares: for convenience, the individual values of  $\sigma$  are shown on the upper axis for a testing temperature of 923 K. When plotted in this form, there is a reasonably good

agreement between the early data and the present results and the H–D region is now reduced to a regime where  $n \approx 3$  rather than  $n = 1$ .

Comparison with experiments showing no evidence for H–D creep

Figure 8 shows the present experimental data as solid points with additional results given as open points which were reported for samples of polycrystalline pure Al where there was no evidence for H–D creep [30, 39, 40]. It is apparent that the two sets of data are in agreement within the power-law creep regime where  $n = 4.5$  but at lower stresses the other data show no evidence for a new creep regime and instead all of the datum points lie on the extrapolation of the line for  $n = 4.5$ .

There are two probable explanations for this difference. First, some of the other results used samples of 99.99% purity [30, 40] which may be insufficient to reveal H–D creep. Second, all of the other tests were conducted in compression using specimens with low aspect ratios equal to, or very close to, 1.0. It is well-known that creep is generally inhibited in these short samples because of the end effects which constitute a large fraction of the samples [32].

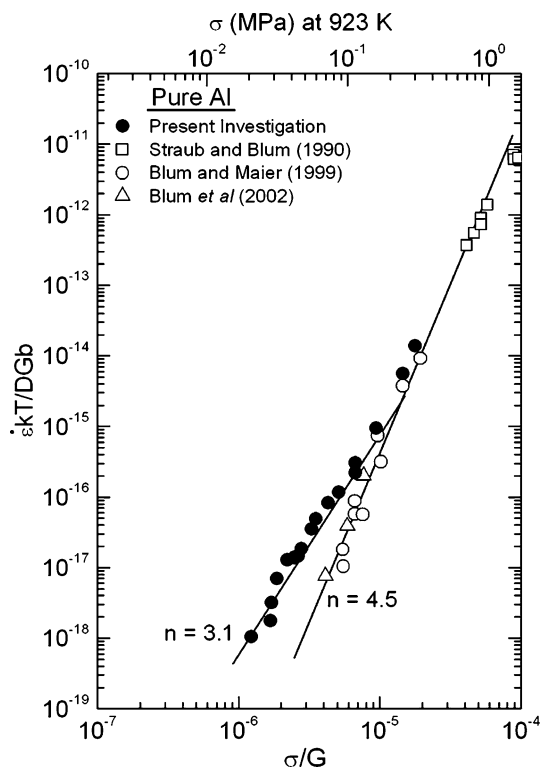


**Fig. 8** Normalized creep rate versus normalized stress for the present investigation and for earlier data showing no evidence for H–D creep [30, 39, 40]

Comparison with experiments showing evidence for H–D creep

The early work of Barrett et al. [13] confirmed the occurrence of H–D creep and reported creep rates that were similar to those reported by Harper and Dorn [12]. These data are plotted in Fig. 9 together with the present results which are again shown as solid points. Although there is some scatter in the experimental points, these results are consistent with the present data except at the two lowest stresses, up to  $\sim 0.03$  MPa, where the measured creep rates are anomalously high.

A second example is shown in Fig. 10 where the instantaneous creep rate reported by Mohamed and Ginter [22] is plotted against strain for a creep test conducted at 923 K using a stress of 0.050 MPa: these results were obtained in double-shear testing and the data were converted to the normal strain rate and normal strain using  $\sigma = 2\tau$  and  $\dot{\epsilon} = 2\dot{\gamma}/3$ . Also shown in Fig. 10 are results obtained from the present experiments, normalized to a temperature of 923 K, for an applied stress of 0.053 MPa. The two vertical lines delineate factors of 2 and 3 on the strain rate axis and it is apparent that these two sets of data are in agreement to within a factor of 3. This agreement is excellent when it is noted that the two different tests were performed on a polycrystalline aluminum using double-

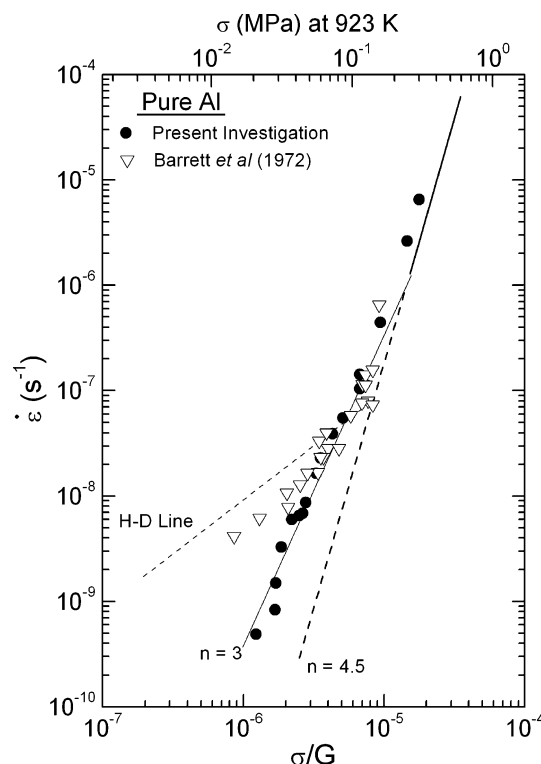


**Fig. 9** Steady-state creep rate versus normalized stress for the present results and the early data of Barrett et al. [13]



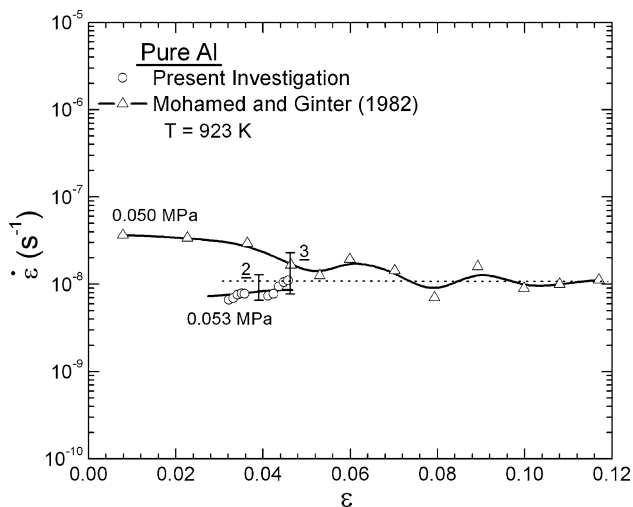


**Fig. 10** Instantaneous strain rate versus strain for a test conducted in the present investigation and early data reported by Mohamed and Ginter [22] normalized to a temperature of 923 K

shear testing and on a single crystal of aluminum tested in compression, respectively. A direct comparison with the data of Mohamed and Ginter [22] is shown in Fig. 11 where the present results are again given by the solid points. These results show excellent agreement for both investigations.

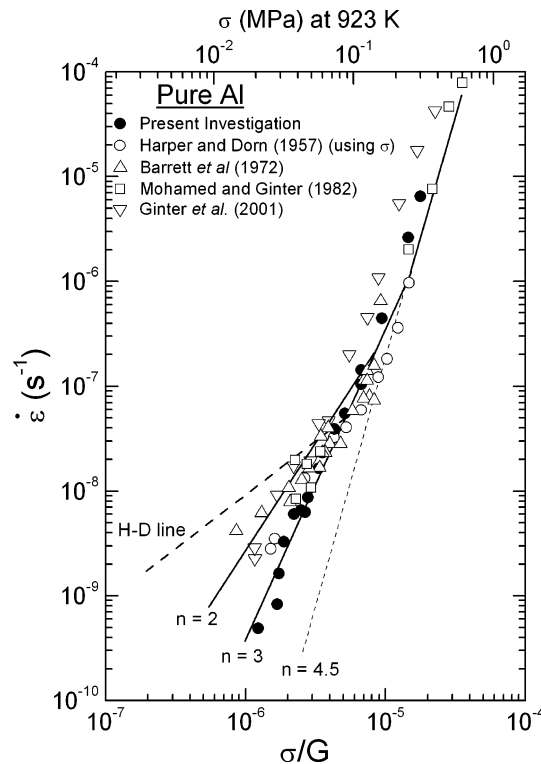


**Fig. 12** Steady-state creep rate versus normalized stress for the present investigation and early data reported by Harper and Dorn [12] where the threshold stress is neglected and Barrett et al. [13], Mohamed and Ginter [22], and Ginter et al. [24]

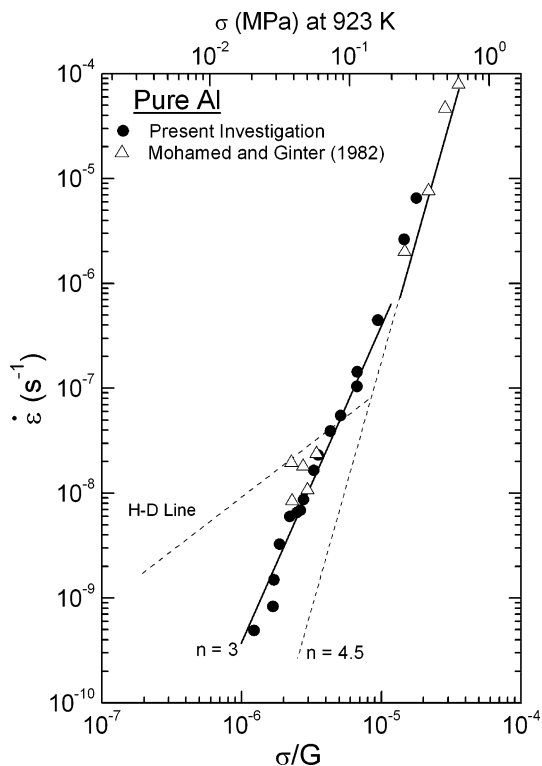


**Fig. 11** Steady-state creep rate versus normalized stress for the present investigation and the early data of Mohamed and Ginter [22]

Finally, it is of interest to compare the present creep data with all of the results available for pure Al to date showing evidence for a change in creep mechanism at the lowest stress levels. This plot is given in Fig. 12 where the present results are denoted by the solid points and the remaining points show the results of Harper and Dorn [12] plotted without including a threshold stress and the later results reported by Barrett et al. [13], Mohamed and Ginter [22] and Ginter et al. [24]. The solid line denotes the transition from  $n = 4.5$  at the higher stresses to an apparent slope of  $n \approx 3$  within the H–D region and the other lines delineate an extrapolation of the line for  $n = 4.5$ , the anticipated behavior for  $n = 2$  and the anticipated behavior with  $n = 1$  based on the original data of Harper and Dorn [12]. All of these results are in reasonable agreement and, despite some scatter in the positions of the individual points, they tend to lie within the range from  $n \approx 2$  to  $n \approx 3$ .

The general conclusion from these experiments is that there is a regime associated with a different creep mechanism when testing very high purity aluminum at high homologous temperatures and very low stresses. Nevertheless, the stress exponent within this region appears to be higher than  $n = 1$  as originally reported by Harper and Dorn [12]. The present results suggest instead that the stress exponent is closer to  $n \approx 3$  within this low stress

region. It is interesting to note that this conclusion is consistent with very recent creep data obtained for other materials suggesting stress exponents  $>1$  at very low stresses in high purity (99.999%) Pb [27] and  $n \approx 2$  in OFHC Cu [26] where both materials were tested at high homologous temperatures.

### Summary and conclusions

1. A series of compressive creep experiments were conducted on very high purity aluminum single crystals to evaluate the role of Harper–Dorn creep at high homologous temperatures. The results confirm the occurrence of a different creep behavior at low applied stresses but with a stress exponent closer to  $n \approx 3$  rather than the traditional value of  $n = 1$ .
2. The dislocation densities measured from etch pits after creep testing within this low stress region are consistent with the behavior anticipated from a direct extrapolation of similar dislocation density data recorded in the conventional power-law region at high stresses.
3. When plotted as the steady-state creep rate against the normalized stress on logarithmic axes, the present results are in good agreement with most of the earlier experimental data for high purity aluminum including with the early results of Harper and Dorn when their data are plotted without including a threshold stress.

**Acknowledgements** We thank Dr. Philip Eisenlohr and Prof. Wolfgang Blum (University of Erlangen–Nürnberg) for several helpful discussions. This work was supported by the Lawrence Livermore Laboratory under Grant B552748.

**Open Access** This article is distributed under the terms of the Creative Commons Attribution Noncommercial License which permits any noncommercial use, distribution, and reproduction in any medium, provided the original author(s) and source are credited.

### References

1. Bird JE, Mukherjee AK, Dorn JE (1969) In: Brandon DG, Rosen A (eds) Quantitative relation between properties and microstructure. Israel Universities Press, Jerusalem, Israel, p 255
2. Langdon TG (2002) Metall Mater Trans 33A:249
3. Weertman J (1957) J Appl Phys 28:1185. doi:10.1063/1.1722604
4. Weertman J (1955) J Appl Phys 26:1213. doi:10.1063/1.1721875
5. Mohamed FA, Langdon TG (1974) Acta Metall 22:779. doi:10.1016/0001-6160(74)90088-1
6. Yavari P, Langdon TG (1982) Acta Metall 30:2181. doi:10.1016/0001-6160(82)90139-0
7. Cannon WR, Langdon TG (1983) J Mater Sci 18:1. doi:10.1007/BF00543808

8. Cannon WR, Langdon TG (1988) J Mater Sci 23:1. doi:10.1007/BF01174028
9. Nabarro FRN (1948) Report of a conference on strength of solids. The Physical Society, London, UK, p 75
10. Herring C (1950) J Appl Phys 21:437. doi:10.1063/1.1699681
11. Coble RL (1963) J Appl Phys 34:1679. doi:10.1063/1.1702656
12. Harper J, Dorn JE (1957) Acta Metall 5:654. doi:10.1016/0001-6160(57)90112-8
13. Barrett CR, Muehleisen EC, Nix WD (1972) Mater Sci Eng 10:33. doi:10.1016/0025-5416(72)90063-8
14. Mohamed FA, Murty KL, Morris JW (1973) Metall Trans 4:935. doi:10.1007/BF02645593
15. Mohamed FA, Langdon TG (1974) Metall Trans 5:2339. doi:10.1007/BF02644014
16. Kumar P, Kassner ME, Langdon TG (2007) J Mater Sci 42:409. doi:10.1007/s10853-006-0782-4
17. Murty KL, Mohamed FA, Dorn JE (1972) Acta Metall 20:1009. doi:10.1016/0001-6160(72)90135-6
18. Murty KL (1974) Mater Sci Eng 14:169. doi:10.1016/0025-5416(74)90010-X
19. Mohamed FA (1978) Metall Trans 9A:1343
20. Yavari P, Mohamed FA, Langdon TG (1981) Acta Metall 29:1495. doi:10.1016/0001-6160(81)90184-X
21. Yavari P, Miller DA, Langdon TG (1982) Acta Metall 30:871. doi:10.1016/0001-6160(82)90085-2
22. Mohamed FA, Ginter TJ (1982) Acta Metall 30:1869. doi:10.1016/0001-6160(82)90027-X
23. Lee S, Ardell AJ (1985) In: McQueen HJ, Bailon J-P, Dickson JJ, Jonas JJ, Akben MG (eds) Strength of metals and alloys (ICSMA 7), vol 1. Pergamon Press, Oxford, UK, p 671
24. Ginter TJ, Chaudhury PK, Mohamed FA (2001) Acta Mater 49:263. doi:10.1016/S1359-6454(00)00316-5
25. Ginter TJ, Mohamed FA (2002) Mater Sci Eng A322:148. doi:10.1016/S0921-5093(01)01127-3
26. Srivastava V, McNee KR, Jones H, Greenwood GW (2005) Mater Sci Tech 21:701
27. Mohamed FA (2007) Mater Sci Eng A463:177. doi:10.1016/j.msea.2006.06.142
28. Muehleisen EC, Barrett CR, Nix WD (1970) Scripta Metall 4:995. doi:10.1016/0036-9748(70)90047-5
29. Burton B (1972) Phil Mag 25:645. doi:10.1080/14786437208228897
30. Blum W, Maier W (1999) Phys Stat Sol (a) 171:467. doi:10.1002/(SICI)1521-396X(199902)171:2<467::AID-PSSA467>3.0.CO;2-8
31. McNee KR, Jones H, Greenwood GW (2001) In: Parker JD (ed) Creep and fracture of engineering materials and structures. The Institute of Materials, London, UK, p 185
32. Evans AG, Langdon TG (1976) Prog Mater Sci 21:171. doi:10.1016/0079-6425(76)90006-2
33. Bailey JE, Hirsch PB (1960) Phil Mag 5:485. doi:10.1080/14786436008238300
34. Horiuchi R, Otsuka M (1972) Trans Japan Inst Metals 13:284
35. Kumar P, Kassner ME, Blum W, Eisenlohr P, Langdon TG (2008) Mater Sci Eng (in press)
36. Kassner ME, McMahon ME (1987) Metall Trans 18A:835
37. Lin P, Lee SS, Ardell AJ (1986) Acta Metall 37:739. doi:10.1016/0001-6160(89)90257-5
38. Blum W (1993) In: Cahn RW, Hassen P, Kramer EJ (eds) Plastic deformation and fracture. VCH Publishers, Weinheim, Germany, p 339
39. Straub S, Blum W (1990) Scripta Metall Mater 24:1837. doi:10.1016/0956-716X(90)90036-G
40. Blum W, Eisenlohr P, Breutingger F (2002) Metall Mater Trans 33A:291